Joint Localization and Channel Estimation for UAV-Assisted Millimeter Wave Communications

George C. Alexandropoulos[†], Evangelos Vlachos[§], and Besma Smida[‡]
[†]Department of Informatics and Telecommunications, National and Kapodistrian University of Athens, Greece
[§]Industrial Systems Institute, ATHENA Research Center, Rio-Patras, Greece
[‡]Department of Electrical and Computer Engineering, University of Illinois at Chicago, USA
e-mails: alexandg@di.uoa.gr, evlachos@isi.gr, smida@uic.edu

2020 54th Asilomar Conference on Signals, Systems, and Computers | 978-0-7381-3126-9/20/$31.00 ©2020 IEEE | DOI: 10.1109/IEEECONF51394.2020.9443514

***Abstract*—In this paper, we consider millimeter Wave (mmWave) communications between an Unmanned Aerial Vehicle (UAV) and a base station. By assuming that both communication nodes are equipped with arrays of multiple antenna elements, we focus on the joint estimation of the UAV position and the Multiple Input Multiple Output (MIMO) channel coefficients. Capitalizing on the line-of-sight signal propagation conditions and the beamspace representation of the wireless channel, we first estimate the UAV position. Using this estimation, we then present a matrix completion formulation for the recovery of the remaining non-line-of-sight components of the MIMO channel matrix, which is efficiently solved via the alternating direction method of multipliers. Selected simulation results for a 28GHz channel model verify that the proposed scheme is beneficial both in terms of estimation accuracy and resources utilization.**

***Index Terms*—Channel estimation, localization, matrix completion, millimeter wave, MIMO, unmanned aerial vehicle.**

I. Introduction

Unmanned Aerial Vehicles (UAVs) are expected to open attractive vertical markets in the telecommunications industry, bringing new revenue opportunities for mobile network vendors and operators in fifth generation (5G) wireless networks, and beyond [1]. High data rate networking between manned vehicles and UAVs can enable real-time sensor fusion, surveillance, and reconnaissance payloads. In addition, UAVs have been proposed as an efficient means to provide communication coverage to areas unreachable by traditional networks [2]–[5], as well as crisis management, where disasters frequently cause communication infrastructure failures [6].

Radio localization and sensing is gaining increased importance in 5G networks [7] enabling various commercial applications, such as personal navigation, indoor localization, and radar sensing [8]. The combination of increased communication bandwidth and larger antenna arrays in 5G has led to improvements in localization accuracy, rendering efficient localization from a single Base Station (BS) possible [9]. This trend is continuing in beyond 5G research, where extremely large bandwidths at carrier frequencies up to 0.1THz are being explored together with transceiver architectures based on extremely massive electromagnetically excited elements [10] (e.g., conventional dipoles and metamaterials), intended for combating pathloss due to small element apertures. The latter factors enable a myriad of new opportunities for radio localization and sensing [11]–[14].

A point-to-point milimeter Wave (mmWave) backhaul communication system with large antenna arrays at both communication ends was considered in [15], where position information available from displacement sensors was shared between the nodes to devised a beam alignment approach with reduced latency. A location-aided strategy, where prior location information allowed to speed up the adaptive channel estimation and beamforming processes was also proposed in [16]. In [17], an algorithm for the joint position and velocity estimation problem in mmWave cloud radio access networks with lens antenna arrays was presented. A mmWave network of multiple UAVs with multiple antennas was considered in [18], where the one acts as an access point and the rest as airborne users, and studied the problem of estimation and tracking of frequency selective channels, leveraging prior information about the positions and trajectories of the UAVs. The positions of two UAVs together with their power control for maximizing their sum-throughput were studied in [19], considering probabilistic Line-Of-Sight (LOS) channel models. Leveraging a variational Bayesian approach in [20], a soft information about the Angle of Arrivals (AoAs) of mmWave receivers was initially obtained, which was then exploited to localize the users and improve the channel estimation performance.

In this paper, we present a joint localization and channel estimation approach for mmWave MIMO communications between a ground BS and a UAV. Leveraging the beamspace representation of the wireless channel, we first estimate the UAV position, which is further exploited in devising a Matrix Completion (MC) formulation and an algorithm for the estimation of the remaining MIMO channel components. It is shown via simulations for a 28GHz channel model that the proposed approach offers satisfactory accuracy with fewer training symbols than selected benchmark techniques.

Notations: Vectors and matrices are denoted by boldface lowercase and boldface capital letters, respectively. The transpose and Hermitian transpose of $\mathbf{A}$ are denoted by $\mathbf{A}^T$ and $\mathbf{A}^H$, respectively, while $[\mathbf{A}]_{i,j}$ is the (i,j)-th element and $[\mathbf{A}]_{i,:}$ is the i-th row of $\mathbf{A}$. $\mathbf{I}_n$ and $\mathbf{0}_n$ are the $n \times n$ identity and zeros' matrices. The Euclidean norm of $\mathbf{a}$ is denoted by $\|\mathbf{a}\|$, whereas $\|\mathbf{A}\|_*$ and $\|\mathbf{A}\|_1$ are $\mathbf{A}$'s nuclear and $L1$ norms, respectively. $\mathbb{R}$ and $\mathbb{C}$ are the real and complex number sets, respectively. $\mathbf{x} \sim \mathcal{CN}(\mathbf{a}, \mathbf{A})$ is a complex Gaussian random vector with mean $\mathbf{a}$ and covariance matrix $\mathbf{A}$, and $\jmath \triangleq \sqrt{-1}$.

II. System and Channel Models

A. System model

We consider a BS equipped with a N_{T}-element Uniform Linear antenna Array (ULA) that wishes to communicate in the mmWave frequency band with a UAV, which possesses a ULA with N_{R} antenna elements. A frame-by-frame communication is assumed, according to which the wireless channel remains constant during each frame, but might change independently from one frame to another. Every frame consists of T time slots dedicated for channel estimation, whereas the rest of the frame is used for data communication. For $\mathbf{P} \in \mathbb{C}^{N_{\mathrm{T}} \times T}$ denoting the BS training symbols in T consecutive slots, the $N_{\mathrm{R}} \times T$ baseband received signal at the UAV is given by

$$\mathbf{Y} = \mathbf{H}\mathbf{P} + \mathbf{N}, \tag{1}$$

where $\mathbf{H} \in \mathbb{C}^{N_{\mathrm{R}} \times N_{\mathrm{T}}}$ is the unknown mmWave MIMO channel, and $\mathbf{N} \in \mathbb{C}^{N_{\mathrm{R}} \times T}$ is the Additive Gaussian complex White Noise (AWGN) distributed as $[\mathbf{N}]_{i,:} \sim \mathcal{CN}(\mathbf{0}_{N_{\mathrm{R}}}, \sigma_n^2 \mathbf{I}_{N_{\mathrm{R}}})$.

In this paper, we propose to spatially sample the unknown channel matrix $\mathbf{H}$ with dedicated training symbols, and then apply MC to recover its missing entries. Let us assume that the $N_{\mathrm{R}} \times N_{\mathrm{T}}$ matrix $\mathbf{\Omega}$ represents the spatial sampling of the received signal, including only zeros and ones, with at least one unit element per column. By considering that the $N_{\mathrm{T}} \times N_{\mathrm{T}}$ diagonal matrices $\mathbf{P}_i \triangleq \mathrm{diag}([\mathbf{\Omega}]_{i,:})$ with $i = 1, 2, \ldots, N_{\mathrm{R}}$ (i.e., $T = N_{\mathrm{T}}$) include the BS training symbols, the spatially sampled noisy version of the unknown channel $\mathbf{H}$ at the UAV is obtained as

$$\mathbf{Y} = \sum_{i=1}^{N_{\mathrm{R}}} \mathbf{E}_i \mathbf{H} \mathrm{diag}([\mathbf{\Omega}]_{i,:}) + \mathbf{\Omega} \circ \mathbf{N}, \tag{2}$$

where $\mathbf{Y} \in \mathbb{C}^{N_{\mathrm{R}} \times N_{\mathrm{T}}}$, $\circ$ represents the Hadamard matrix product, and each $N_{\mathrm{R}} \times N_{\mathrm{R}}$ matrix $\mathbf{E}_i$ has zeros' entries except its (i,i)-th element that is unity. Using properties of the Hadamard product, (2) can be re-written as

$$\mathbf{Y} = \mathbf{\Omega} \circ (\mathbf{H} + \mathbf{N}), \tag{3}$$

which indicates our proposed spatial sampling realized with $K \triangleq \sum_{i=1}^{N_{\mathrm{R}}} \sum_{j=1}^{N_{\mathrm{T}}} [\mathbf{\Omega}]_{i,j}$ training symbols in N_{T} time slots.

B. Channel Model

We adopt the statistical spatial channel model of [21] for the considered mmWave MIMO wireless channel. This model is based on the time-cluster spatial-lobe assumption, according to which the channel comprises multipath components that travel close in time, and that arrive from potentially different directions in a short propagation time window. The spatial lobes represent main directions of arrival (or departure), where energy arrives over several hundred of nanoseconds. The matrix with the wireless channel gains is modeled as follows:

$$\mathbf{H} = \sqrt{\frac{N_{\mathrm{T}} N_{\mathrm{R}}}{N_p}} \sum_{\ell=1}^{N_p} h_\ell \mathbf{a}_{\mathrm{R}}(\theta_\ell) \mathbf{a}_{\mathrm{T}}^H(\phi_\ell), \tag{4}$$

where h_ℓ is the channel gain of the ℓ-th channel propagation path with $\ell = 1, 2, \ldots, N_p$ and $h_\ell \sim \mathcal{CN}(0, \sigma_\ell^2)$. The variance σ_ℓ^2 of each ℓ-th channel gain depends on the loss imposed by the propagation distance, d, and the carrier frequency, f_c. In mathematical terms, each of these variances is given by:

$$\sigma_\ell^2 = \frac{\gamma_\ell}{\left(\frac{4\pi f_c}{c}\right) d_\ell^{\xi_\ell}}, \tag{5}$$

where ξ_ℓ is the pathloss exponent, c is the speed of light, γ_ℓ denotes the gain, and $\lambda \triangleq c/f_c$ is the carrier wavelength. Also, in (4), the vector $\mathbf{a}_{\mathrm{R}}(\theta_\ell) \in \mathbb{C}^{N_{\mathrm{R}} \times 1}$ denotes the N_{R}-element response vector of the ULA at the UAV at the AoA θ_ℓ of the ℓ-th propagation path. The response vector of the BS's ULA at the Angle of Departure (AoD) ϕ_ℓ of the ℓ-th path is represented by $\mathbf{a}_{\mathrm{T}}(\phi_\ell) \in \mathbb{C}^{N_{\mathrm{T}} \times 1}$. The latter ULA response vectors are defined at any incoming/outgoing angle θ as:

$$\mathbf{a}(\theta) = \frac{1}{\sqrt{N}} [1\, e^{\jmath \pi \frac{d}{\lambda} \sin(\theta)}\, e^{\jmath 2\pi \sin(\theta)}\, \cdots\, e^{\jmath (N-1)\pi \frac{d}{\lambda} \sin(\theta)}]^T. \tag{6}$$

In the considered system model (4), we assume that the first channel propagation path, i.e., for $\ell = 1$, represents the Line-Of-Sight (LOS) path. Using the notation $\mathbf{p}_{\mathrm{uav}} \triangleq [x_{\mathrm{uav}}\, y_{\mathrm{uav}}]^T \in \mathbb{R}^{2\times 1}$ for the position of the UAV and $\mathbf{p}_{\mathrm{bs}} \triangleq [x_{\mathrm{bs}}\, y_{\mathrm{bs}}]^T \in \mathbb{R}^{2\times 1}$ for the BS position, the distance between these two nodes can be calculated as:

$$d_1 = \|\mathbf{p}_{\mathrm{bs}} - \mathbf{p}_{\mathrm{uav}}\|. \tag{7}$$

Hence, the AoA of the LOS path can be easily obtained as

$$\theta_1 = \arctan\left(\frac{y_{\mathrm{uav}} - y_{\mathrm{bs}}}{x_{\mathrm{uav}} - x_{\mathrm{bs}}}\right). \tag{8}$$

III. Joint Localization and Channel Estimation

According to the channel model (4), the first propagation channel path represents the LOS component and the remaining ones the Non-LOS (NLOS) channel components, i.e.:

$$\mathbf{H} = \underbrace{h_1 \mathbf{a}_{\mathrm{R}}(\theta_1) \mathbf{a}_{\mathrm{T}}^H(\phi_1)}_{\triangleq \mathbf{H}_{\mathrm{LOS}}} + \underbrace{\sum_{\ell=2}^{N_p} h_\ell \mathbf{a}(\theta_\ell) \mathbf{a}_{\mathrm{T}}^H(\phi_\ell)}_{\triangleq \mathbf{H}_{\mathrm{NLOS}}}. \tag{9}$$

Given the fact that for $\mathbf{H}$'s rank holds $\mathrm{rank}(\mathbf{H}) = N_p$, it follows that $\mathrm{rank}(\mathbf{H}_{\mathrm{LOS}}) = 1$ and $\mathrm{rank}(\mathbf{H}_{\mathrm{NLOS}}) = N_p - 1$. By using the virtual representation of the multipath channel in the beamspace domain [21], the MIMO matrix in (9) can be tightly approximated by the following decomposition:

$$\hat{\mathbf{H}} = \underbrace{\mathbf{D}_{\mathrm{R}} \mathbf{S}_{\mathrm{LOS}} \mathbf{D}_{\mathrm{T}}^H}_{\triangleq \hat{\mathbf{H}}_{\mathrm{LOS}}} + \underbrace{\mathbf{D}_{\mathrm{R}} \mathbf{S}_{\mathrm{NLOS}} \mathbf{D}_{\mathrm{T}}^H}_{\triangleq \hat{\mathbf{H}}_{\mathrm{NLOS}}}, \tag{10}$$

where $\mathbf{D}_{\mathrm{R}} \in \mathbb{C}^{N_{\mathrm{R}} \times N_{\mathrm{R}}}$ and $\mathbf{D}_{\mathrm{T}} \in \mathbb{C}^{N_{\mathrm{T}} \times N_{\mathrm{T}}}$ are Discrete Fourier Transform (DFT) matrices referring to the receiver and transmitter sides, respectively, while $\mathbf{S}_{\mathrm{LOS}} \in \mathbb{C}^{N_{\mathrm{R}} \times N_{\mathrm{T}}}$ and $\mathbf{S}_{\mathrm{NLOS}} \in \mathbb{C}^{N_{\mathrm{R}} \times N_{\mathrm{T}}}$ include the channel gains of the channel's LOS and NLOS components, respectively. The matrices $\hat{\mathbf{H}}$, $\hat{\mathbf{H}}_{\mathrm{LOS}}$, and $\hat{\mathbf{H}}_{\mathrm{NLOS}}$ represent the discretized versions of $\mathbf{H}$, $\mathbf{H}_{\mathrm{LOS}}$, and $\mathbf{H}_{\mathrm{NLOS}}$, respectively.

A. UAV Position Information

Given the beamspace representation in (10), the position of the largest channel gain in $\mathbf{S}_{\mathrm{LOS}}$ in conjunction with the DFT beam codebooks $\mathbf{D}_{\mathrm{R}}$ and $\mathbf{D}_{\mathrm{T}}$ provide estimations for the AoA and AoD, respectively, of the LOS component. Supposing that the matrix index of this component is $(i_{\mathrm{LOS}}, j_{\mathrm{LOS}})$, the angles θ_1 and ϕ_1 can be, respectively, estimated as follows:

$$\hat{\theta}_1 = \arcsin\left(\frac{\lambda\,(i_{\mathrm{LOS}}-1)}{d_{\mathrm{ant}}N_{\mathrm{R}}}\right), \tag{11}$$

$$\hat{\phi}_1 = \arcsin\left(\frac{\lambda\,(j_{\mathrm{LOS}}-1)}{d_{\mathrm{ant}}N_{\mathrm{T}}}\right), \tag{12}$$

where d_{ant} denotes the common antenna spacing at the BS and UAV sides. Therefore, extracting the AoA and AoD from the beamspace of the LOS component, can be considered as an extra modality, along with other measurements from the UAV's on-board sensors, e.g., measurements from the Inertial Measurement Unit (IMU) and Global Positioning System (GPS). Note that multi-modal localization permits a more accurate and robust estimation of the UAV's position [22].

Hence, the position of the UAV in the coordinate system, where the BS lies in the origin, can be calculated as:

$$\hat{x}_{\mathrm{uav}} = d_1 \sin(\hat{\theta}_1), \tag{13}$$

$$\hat{y}_{\mathrm{uav}} = d_1 \cos(\hat{\theta}_1), \tag{14}$$

where the distance d_1 between the UAV and BS can be accurately measured in practice using distance-based pathloss, or information from the IMU or the GPS [23].

B. LOS Channel Component Estimation

Let us now consider the case where the UAV position estimation $\hat{\mathbf{p}}_{\mathrm{uav}} = [\hat{x}_{\mathrm{uav}}\ \hat{y}_{\mathrm{uav}}]^T$ and its orientation angle ω are available using UAV on-board sensors. Then, the estimation for the AoA and AoD, respectively, of the LOS channel component can be obtained as:

$$\bar{\theta}_1 = \sin\left(\arctan\left(\frac{\hat{y}_{\mathrm{uav}}}{\hat{x}_{\mathrm{uav}}}\right)\right), \tag{15}$$

$$\bar{\phi}_1 = \frac{\pi}{2} - \omega - \bar{\theta}_1. \tag{16}$$

Using these expressions, the rank-one matrix obtained from the respective steering vectors and referring to the LOS component estimation is $\mathbf{M}_{\mathrm{LOS}} \triangleq \mathbf{a}_{\mathrm{R}}(\bar{\theta}_1)\mathbf{a}_{\mathrm{T}}^H(\bar{\phi}_1)$. Hence, to estimate the actual LOS matrix $\mathbf{H}_{\mathrm{LOS}}$ in (9), we also have to recover the complex channel gain coefficient h_1. We formulate the following optimization problem for the estimation of h_1:

$$\bar{h}_1 \triangleq \arg\min_{x\in\mathbb{C}} \|\mathbf{Y}_1 - x\mathbf{M}_{\mathrm{LOS}}\|^2 \text{ s.t. } |x| \le [\mathbf{\Sigma}]_{1,1}, \tag{17}$$

where $\mathbf{Y} = \mathbf{U}\mathbf{\Sigma}\mathbf{V}^H$ represents the Singular Value Decomposition (SVD) of $\mathbf{Y}$ with $[\mathbf{\Sigma}]_{1,1} \in \mathbb{R}$ being the largest singular value, and $\mathbf{Y}_1 \in \mathbb{C}^{N_{\mathrm{R}}\times N_{\mathrm{T}}}$ is defined as $\mathbf{Y}_1 \triangleq [\mathbf{\Sigma}]_{1,1}\mathbf{U}_1\mathbf{V}_1^H$ with subscript 1 denoting the first column of the respective matrices. The solution of (17) can be efficiently obtained via the available software packages on convex optimization (e.g., CVX , Mosek [24]). Finally, using $\hat{h}_1$ and $\mathbf{M}_{\mathrm{LOS}}$, the LOS channel component $\mathbf{H}_{\mathrm{LOS}}$ can be estimated as

$$\bar{\mathbf{H}}_{\mathrm{LOS}} = \bar{h}_1\mathbf{a}_{\mathrm{R}}(\bar{\theta}_1)\mathbf{a}_{\mathrm{T}}^H(\bar{\phi}_1). \tag{18}$$

The aforementioned steps are summarized in Algorithm 1.

Algorithm 1 Estimation of $\mathbf{H}_{\mathrm{LOS}}$.

Input: $\mathbf{Y}$, $\hat{x}_{\mathrm{uav}}$, $\hat{y}_{\mathrm{uav}}$, and ω
Output: $\bar{\mathbf{H}}_{\mathrm{LOS}}$

1: Compute $\bar{\theta}_1$ using (15).
2: Compute $\bar{\phi}_1$ using (16).
3: Calculate $\mathbf{M}_{\mathrm{LOS}} = \mathbf{a}_{\mathrm{R}}(\bar{\theta}_1)\mathbf{a}_{\mathrm{T}}^H(\bar{\phi}_1)$.
4: Perform $[\mathbf{U}, \mathbf{S}, \mathbf{V}] = \mathrm{SVD}(\mathbf{Y})$.
5: Compute $\mathbf{Y}_1 = [\mathbf{S}]_{1,1}\mathbf{U}_1\mathbf{V}_1^H$.
6: Solve (17) for $\bar{h}_1$.
7: Compute $\bar{\mathbf{H}}_{\mathrm{LOS}} = \bar{h}_1\mathbf{M}_{\mathrm{LOS}}$.

C. NLOS Channel Component Estimation

Suppose that the channel component $\mathbf{H}_{\mathrm{LOS}}$ is known, or estimated as in the previous section. Then, its effect can be removed from the overall channel $\mathbf{H}$, yielding the NLOS channel component: $\mathbf{H}_{\mathrm{NLOS}} = \mathbf{H} - \mathbf{H}_{\mathrm{LOS}}$. When doing so, the estimation of $\mathbf{H}_{\mathrm{NLOS}}$ will require fewer training symbols than estimating $\mathbf{H}$. This holds because $\mathbf{H}_{\mathrm{NLOS}}$ has less degrees of freedom than $\mathbf{H}$; for $\mathbf{H}_{\mathrm{NLOS}}$ holds $\mathrm{rank}(\mathbf{H}_{\mathrm{NLOS}}) = L - 1$.

We assume that the NLOS channel matrix can be well approximated with the discretized version $\hat{\mathbf{H}}_{\mathrm{NLOS}}$, as shown in (10). To estimate $\mathbf{H}_{\mathrm{NLOS}}$, we exploit the low-rank and sparsity properties of the beamspace channel gain matrix $\mathbf{S}_{\mathrm{NLOS}}$ [25], and formulate the following optimization problem:

$$\begin{aligned}\min_{\mathbf{H}_{\mathrm{NLOS}},\,\mathbf{S}_{\mathrm{NLOS}}} \ & \tau_1\|\mathbf{H}_{\mathrm{NLOS}}\|_* + \tau_2\|\mathbf{S}_{\mathrm{NLOS}}\|_1 \\ \text{s.t. } & \mathbf{H}_{\mathrm{NLOS}} = \mathbf{D}_{\mathrm{R}}\mathbf{S}_{\mathrm{NLOS}}\mathbf{D}_{\mathrm{T}}^H, \\ & \mathbf{\Omega}\circ\mathbf{H}_{\mathrm{NLOS}} = \mathbf{\Omega}\circ(\mathbf{Y} - \bar{\mathbf{H}}_{\mathrm{LOS}}),\end{aligned} \tag{19}$$

where $\tau_1, \tau_2 > 0$ and $\mathbf{Y}$ is obtained from (3). This problem can be solved optimally using the Alternating Direction Method of Multipliers (ADMM). A similar approach has been adopted in [25], [26] under different problem formulations. The detailed solution of (19) is omitted due to space limitations.

Finally, supposing that $\bar{\mathbf{H}}_{\mathrm{NLOS}}$ solves (19) for the estimation of $\mathbf{H}_{\mathrm{NLOS}}$, the estimation for $\mathbf{H}$ is $\bar{\mathbf{H}} = \bar{\mathbf{H}}_{\mathrm{LOS}} + \bar{\mathbf{H}}_{\mathrm{NLOS}}$.

IV. Simulation Results

In this section, we evaluate the performance of the proposed position-aided MC approach. We have considered mmWave communications at $f_c = 28$GHz with BS transmit power at 30dB, where the gain of the LOS component is $\gamma_1 = 1$ and the gain of ℓ-th NLOS component, with $\ell = 2, 3, \ldots, N_p$, is $\gamma_\ell = 0.1$. Starting with the recovery of the LOS component given the availability of the UAV position information, we solve (17) for the unknown LOS channel gain and then (18). In Fig. 1, we plot the estimation error over the AWGN power level at the UAV side for $N_p = \{1, 4, 8\}$. We have specifically simulated the Normalized Mean Squared Error

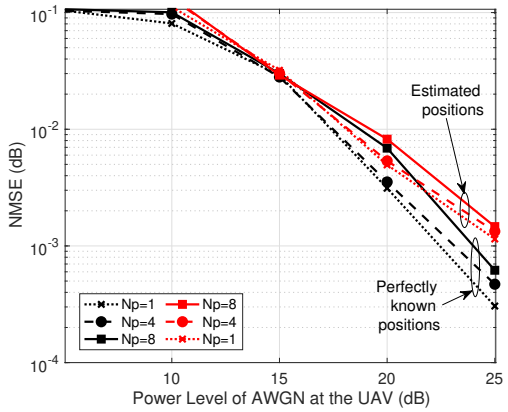

Fig. 1. NMSE in dB of the LOS component estimation for a 32×32 MIMO system over the power level of the AWGN in dB at the UAV side.

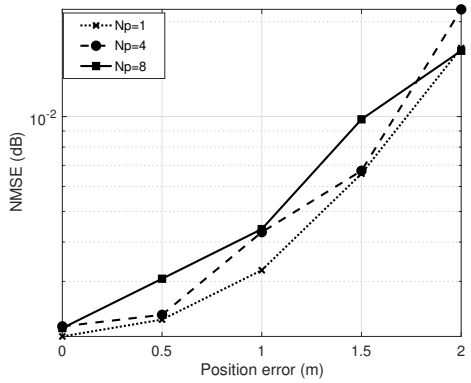

Fig. 2. NMSE in dB of the LOS component estimation for a 32×32 MIMO system with the AWGN power level set to 25dB as a function of the position error in meters.

(NMSE) for the LOS estimation, which is defined as NMSE $\triangleq 10\log_{10}\left(\left(\|\mathbf{S}_{\rm LOS}-\bar{\mathbf{S}}_{\rm LOS}\|\right)/\|\mathbf{S}_{\rm LOS}\|\right)$, where $\bar{\mathbf{S}}_{\rm LOS}$ denotes the estimation for the LOS channel gain. The obtained results verify that, by exploiting the position information, it is possible to achieve low NMSE with significantly small training length. In particular, $T = N_{\rm T} = 32$ training blocks were sufficient for recovering the $N_{\rm R}N_{\rm T} = 1024$ unknown terms of the LOS component matrix. As shown, the N_p value has very small impact on the NMSE performance. Within this figure, we also sketch the performance for the case where the UAV position has been estimated via measurements from on-board sensors [23]. We have actually assumed a 0.5m position error. It can be observed that, at this case for 25dB AWGN power level and $N_p = 4$, the NMSE increases around 3.5dB. In Fig. 2, we further investigate the estimation performance over the position error due to measurement and reconstruction faults. It is shown that, as the position error increases, the NMSE gets significantly impacted.

In Figs. 3(a) and 3(b), the UAV position estimation is depicted for the case where the BS is placed at the origin $(0, 0)$, while the UAV is located at the point $(30\text{m}, 31\text{m})$. For the ideal case where $\mathbf{H}_{\rm LOS}$ was assumed to be perfectly

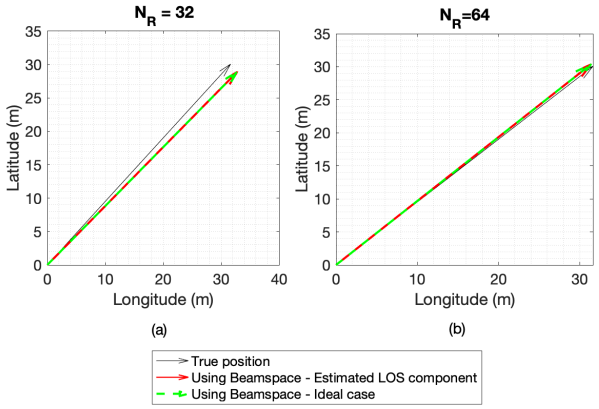

Fig. 3. The UAV positioning vector for $T = 32$, $N_p = 4$, and 15dB for the ratio of the transmit power over the AWGN variance.

known, we have calculated the UAV position as follows. First, we transformed $\mathbf{H}_{\rm LOS}$ in the beamspace domain, yielding the decomposition $\mathbf{S}_{\rm LOS} = \mathbf{D}_{\rm R}^H\mathbf{H}_{\rm LOS}\mathbf{D}_{\rm T}$. Then, we searched for the element inside $\mathbf{S}_{\rm LOS}$ having the largest channel gain, i.e., we solved the the following problem:

$$(i_{\rm LOS}, j_{\rm LOS}) = \max_{(i,j)}[\mathbf{S}_{\rm LOS}]_{i,j}, \tag{20}$$

and finally used (11)–(14) for the position estimation $\hat{\mathbf{p}}_{\rm uav}$. For the estimated LOS component case, we first obtained $\bar{\mathbf{H}}_{\rm LOS}$ from (18) and then followed similar steps to the ideal case. As shown from these two figures, the positioning accuracy using the beamspace representation of the LOS component is less than 2m for the case of a 32×32 system and less than 1m for a 64×64 system.

The recovery of the overall channel matrix $\mathbf{H}$ for the case where the AOA θ_1, the AoD ϕ_1, and the gain h_1 of the LOS channel component are known is illustrated in Fig. 4. In this figure, we have simulated the NMSE performance in dB versus K and for $N_p = \{1, 4, 8\}$ of the following channel estimation techniques: *i*) the conventional MC technique, where the problem (19) was solved without any side information, using K non-zero training samples represented by the ones in the matrix $\mathbf{\Omega}$; *ii*) the LOS component only technique, where we have considered that the LOS component $\mathbf{H}_{\rm LOS}$ is known, and reconstructed the overall channel as $\mathbf{H} = \mathbf{H}_{\rm LOS}$; *iii*) the position-aided MC technique, where the problem (19) was solved via ADMM; and *iv*) the position-aided MC-L1 technique, where the problem (19) was solved via ADMM exploiting the low-dimensionality of the eigenspace and the beamspace of the unknown channel. As shown from the figure, the LOS component only technique is not able to achieve low NMSE for the cases where $N_p > 1$. This happens because the effect of the multiple propagation paths is non-negligible. However, for $N_p = 1$, this technique achieves similar performance to the proposed ones. It is also shown that the conventional MC technique converges slow with the number of the training symbols K. This is due to the fact that this technique does not exploit the information regarding

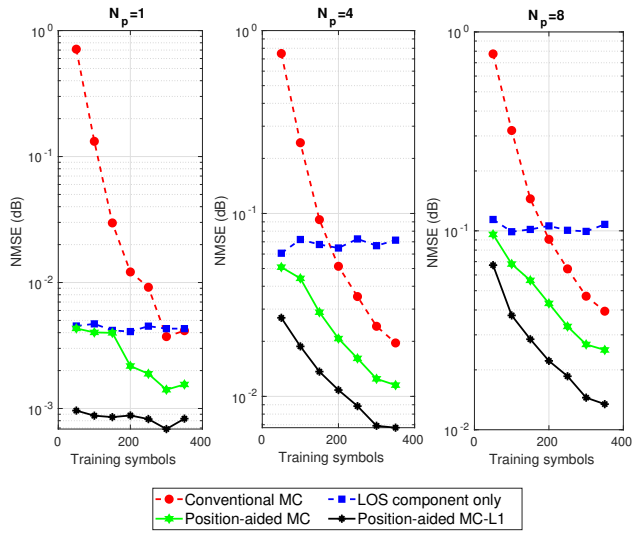

Fig. 4. NMSE in dB versus the number of training symbols K for various channel estimation algorithms and different values for N_p.

the position, thus, a larger number of unknowns has to be recovered. Evidently, the position-aided MC exploits the given information about the LOS component, hence, fewer unknowns for the channel matrix need to be estimated. This technique converges faster than the conventional MC requiring smaller training lengths for all considered values for N_p. The best performance among the considered techniques is achieved from the position-aided MC-L1 technique, which exploits simultaneously the sparsity of the beamspace $\mathbf{S}_{\text{NLOS}}$, and the low-rank property of the spatial channel matrix $\mathbf{H}_{\text{NLOS}}$. This technique is more robust to cases where N_p is large, i.e., for cases with increased numbers of propagation paths, thus, higher number of unknowns need to be determined.

V. Conclusion

In this paper, we investigated the problem of joint localization and channel estimation for UAV-assisted mmWave massive MIMO communications. Capitalizing on the LOS signal propagation and the beamspace representation of the wireless channel, we designed a UAV position estimation technique. We then proposed a technique for the recovery of the LOS channel component exploiting the UAV position estimation, while the recovery of the NLOS channel component was achieved via a MC-based problem formulation, which was solved efficiently via ADMM. Our representative simulation results showcased that the proposed approach outperforms the considered baselines with fewer channel training lengths.

References

[1] Y. Zeng, Q. Wu, and R. Zhang, "Accessing from the sky: A tutorial on UAV communications for 5G and beyond," *Proc. IEEE*, vol. 107, no. 12, pp. 2327–2375, Dec. 2019.

[2] D. W. Matolak, "Air-ground channels & models: Comprehensive review and considerations for unmanned aircraft systems," in *Proc. IEEE Aerospace Conf.*, Big Sky, USA, Mar. 2012, pp. 1–17.

[3] E. W. Frew and T. X. Brown, "Airborne communication networks for small unmanned aircraft systems," *Proc. IEEE*, vol. 96, no. 12, pp. 2008–2027, Dec. 2008.

[4] S. Chandrasekharan *et al.*, "Designing and implementing future aerial communication networks," *IEEE Commun. Mag.*, vol. 54, no. 17, pp. 26–34, May 2016.

[5] L. Zeng, X. Cheng, C.-X. Wang, and X. Yin, "A 3D geometry-based stochastic channel model for UAV-MIMO channels," in *Proc. IEEE WCNC*, San Francisco, USA, Mar. 2017, pp. 1–6.

[6] Y. Zeng, R. Zhang, and T. J. Lim, "Wireless communications with unmanned aerial vehicles: Opportunities and challenges," *IEEE Commun. Mag.*, vol. 54, no. 5, pp. 36–42, May 2016.

[7] R. D. Taranto *et al.*, "Location-aware communications for 5G networks: How location information can improve scalability, latency, and robustness of 5G," *IEEE Signal Process. Mag.*, vol. 31, no. 6, pp. 102–112, Nov. 2014.

[8] R. Keating, M. Säily, J. Hulkkonen, and J. Karjalainen, "Overview of positioning in 5G new radio," in *Proc. IEEE ISWCS*, Oulu, Finland, Aug. 2019.

[9] A. Shahmansoori, G. E. Garcia, G. Destino, G. Seco-Granados, and H. Wymeersch, "Position and orientation estimation through millimeter-wave MIMO in 5G systems," *IEEE Trans. Wireless Commun.*, vol. 17, no. 3, pp. 1822–1835, Mar. 2018.

[10] "The next hyper-connected experience for all," White Paper, Samsung 6G Vision, Jun. 2020.

[11] G. C. Alexandropoulos, R. Khayatzadeh, M. Kamoun, Y. Ganghua, and M. Debbah, "Indoor time reversal wireless communication: Experimental results for localization and signal coverage," in *Proc. IEEE ICASSP*, Brighton, UK, May 2019.

[12] C. Huang, G. C. Alexandropoulos, C. Yuen, and M. Debbah, "Indoor signal focusing with deep learning designed reconfigurable intelligent surfaces," in *Proc. IEEE SPAWC*, Cannes, France, Jul. 2019, pp. 1–6.

[13] C. Xiang, S. Zhang, S. Xu, S. Cao, G. C. Alexandropoulos, and V. K. N. Lau, "Robust sub-meter level indoor localization with a single WiFi access point– Regression versus classification," *IEEE Access*, vol. 7, no. 1, pp. 146 309–146 321, Dec. 2019.

[14] A. Bourdoux *et al.*, "6G white paper on localization and sensing," *arXiv preprint arXiv:2006.01779*, 2020.

[15] G. C. Alexandropoulos, "Position aided beam alignment for millimeter wave backhaul systems with large phased arrays," in *Proc. IEEE CAMSAP*, Curaçao, Dutch Antilles, Dec. 2017, pp. 1–5.

[16] N. Garcia, H. Wymeersch, E. G. Ström, and D. T. Slock, "Location-aided mm-wave channel estimation for vehicular communication," in *Proc. IEEE SPAWC*, Edinburgh, UK, Jul. 2016, pp. 1–6.

[17] J. Yang, S. Jin, Y. Han, M. Matthaiou, and Y. Zhu, "3-D position and velocity estimation in 5G mmWave CRAN with lens antenna arrays," in *Proc. IEEE VTC-Fall*, Honolulu, USA, Sep. 2019, pp. 1–6.

[18] J. Rodriguez-Fernandez, N. Gonzalez-Prelcic, and J. Robert W. Heath, "Position-aided compressive channel estimation and tracking for millimeter wave multi-user MIMO air-to-air communications," in *Proc. IEEE ICC*, Kansas, USA, May 2018, pp. 1–6.

[19] X. Li and J. Xu, "Positioning optimization for sum-rate maximization in UAV-enabled interference channel," *IEEE Signal Process. Lett.*, vol. 26, no. 10, pp. 1466–1470, Oct. 2019.

[20] X. Yang, C. K. Wen, S. Jin, A. L. Swindlehurst, and J. Zhang, "Joint channel estimation and localization for cooperative millimeter wave systems," in *Proc. IEEE SPAWC*, Atlanta, USA, Jul. 2020, pp. 1–6.

[21] O. E. Ayach, S. Rajagopal, S. Abu-Surra, Z. Pi, and R. W. Heath, "Spatially sparse precoding in millimeter wave MIMO systems," *IEEE Trans. Wireless Commun.*, vol. 13, no. 3, pp. 1499–1513, 2014.

[22] N. Piperigkos, A. S. Lalos, K. Berberidis, and C. Anagnostopoulos, "Cooperative multi-modal localization in connected and autonomous vehicles," in *Proc. IEEE CAVS*, Victoria, Canada, Nov. 2020, pp. 1–6.

[23] N. Souli, P. Kolios, and G. Ellinas, "Relative positioning of autonomous systems using signals of opportunity," in *Proc. IEEE VTC-Spring*, Antwerp, Belgium, May 2020, pp. 1–6.

[24] M. Grant and S. Boyd, "CVX: Matlab software for disciplined convex programming, version 2.1," http://cvxr.com/cvx, Mar. 2014.

[25] E. Vlachos, G. C. Alexandropoulos, and J. Thompson, "Wideband MIMO channel estimation for hybrid beamforming millimeter wave systems via random spatial sampling," *IEEE J. Sel. Topics Signal Process.*, vol. 13, no. 5, pp. 1136–1150, Sep. 2019.

[26] E. Vlachos, G. C. Alexandropoulos, and J. Thompson, "Massive MIMO channel estimation for millimeter wave systems via matrix completion," *IEEE Signal Process. Lett.*, vol. 25, no. 11, pp. 1675–1679, Nov. 2018.